Photoluminescence Spectroscopy of Thermal Donors and Oxygen Precipitates Formed in Czochralski Silicon at 450 °C

Manjula Siriwardhana, Fiacre Rougieux, Rabin Basnet, Hieu T. Nguyen, and Daniel Macdonald

***Abstract*—Photoluminescence spectra have been measured at 80 K in Czochralski-grown silicon wafers annealed at 450 °C, causing thermal donor and oxygen-precipitate generation. Six subbandgap luminescence peaks were identified after the annealing. One peak, centered at 1206 nm, was found to increase with a similar time constant to the thermal donor concentration measured by changes in the resistivity. We propose that the other five peaks are related to the formation of oxygen precipitates (OPs), or their nuclei. These peaks remain after a thermal donor annihilation (TDA) step, while the 1206 nm peak disappeared. This is consistent with our previous observations that the growth of OPs occurs concurrently with the growth of thermal donors at low temperatures. The annihilation of the thermal donors leads to an incomplete recovery of the interstitial oxygen concentration, consistent with the formation of precipitates. Recombination-active ring-defects formed during the annealing also remain after TDA.**

***Index Terms*—Oxygen precipitate (OP), photoluminescence, point defects, silicon, thermal donors.**

I. Introduction

OXYGEN and carbon are two of the most common impurities in electronic-grade and solar-grade silicon. Low-temperature annealing, near 450 °C, produces a wide variety of electrically-active defects in Czochralski-grown Si containing high concentrations of interstitial oxygen [O_i], including thermal donors [1]. Their structure depends on the annealing process, prior thermal history of the sample, and the concentration of O_i (and C_s) in the starting material [2]. Thermal donors act as shallow double donors, and can therefore alter the material resistivity. Such thermal double donors (TDDs) and oxygen precipitates (OPs) can be detrimental to solar cell efficiency. The generation and characterization of TDDs has been intensively studied over the past 50 years [3]. Previous studies have shown that thermal donors can act as trapping centers [4], [5] or recombination centers [6] and are detrimental to silicon heterojunction solar cells [6]. However, recent results have shown that thermal donors may not be the only cause of lifetime degradation during annealing of Cz- Si wafers at 450 °C [7], as the formation of OPs, or at least precipitate nuclei, can occur even at these low temperatures. This work aims to clarify the growth of OPs and thermal donor species during 450 °C annealing via analyzing subband-gap peaks in photoluminescence spectra, coupled with complementary measurements of changes in [O_i], resistivity and carrier lifetime. The work further demonstrates that photoluminescence spectra measured at 80 K can provide a powerful way to study and identify the defects generated by TDDs and OPs

Manuscript received August 26, 2021; revised September 30, 2021; accepted October 29, 2021. Date of publication November 23, 2021; date of current version December 23, 2021. This work was supported in part by the Australian Renewable Energy Agency under project RND016, RND017, and Project 1-A060 and in part by the Australian Centre for Advanced Photovoltaics. The work of Hieu T. Nguyen was supported by the Australian Centre for Advanced Photovoltaics. *(Corresponding author: Manjula Siriwardhana.)*

Manjula Siriwardhana, Rabin Basnet, Hieu T. Nguyen, and Daniel Macdonald are with the School of Engineering, The Australian National University, Canberra, ACT 2601, Australia (e-mail: mtsiriwardhana@gmail.com; rabin.basnet@anu.edu.au; hieu.nguyen@anu.edu.au; daniel.macdonald@anu.edu.au).

Fiacre Rougieux is with the School of Photovoltaic and Renewable Energy Engineering, University of New South Wales, Sydney, NSW 2052, Australia (e-mail: fiacre.rougieux@unsw.edu.au).

Color versions of one or more figures in this article are available at https://doi.org/10.1109/JPHOTOV.2021.3126120.

Digital Object Identifier 10.1109/JPHOTOV.2021.3126120

II. Background

TDDs form a family of defects consisting of chains of oxygen atoms, labeled TDD(1), TDD(2) ….TDD(N) [6]. Depending on the annealing temperature and the duration of annealing, at least seventeen different configurations of TDDs have been reported in Cz silicon wafers annealed in the temperature range 350 °C–550 °C [8]. TDD(N + 1) is generated from TDD(N) by the addition of one extra oxygen atom [1] with each TDD(N) having slightly different ionization energy levels [1], [9]–[11]. During the thermal donor growth process, the concentration of each species reaches a maximum and then decays [12]. The initial rate of donor formation has been found to be approximately proportional to the fourth power of the initial oxygen concentration [12]. Although much has been learnt about TDDs, their exact chemical composition and various optical, electronic and structural properties remain unclear. Recent work revealed (via minority carrier lifetime and interstitial oxygen measurements) that oxygen precipitation (OP) occurs concurrently with thermal donor growth during low temperature annealing of silicon [7]. These OPs also introduce recombination active defects in silicon. The recombination activity of OPs is a function of their strain, decoration by metallic impurities, and surrounding defects, such as dislocations or stacking faults [13]. Claybourn and Newman found that during annealing at 450 °C, approximately 13 oxygen atoms are lost from the solution during the time

TABLE I
SUMMARY OF PREVIOUSLY REPORTED PL PEAKS RELATED TO THERMAL DONORS OR OXYGEN PRECIPITATION

Peak energy (eV)	Peak wavelength (nm)	Anneal temperature (°C) / time (hours)	Measurement temperature (K)	Reference
0.767	1617	450°C	77K	Tajima *et al*., 1983 [28]
0.7 broad peak	1771	470°C, 64 h	Room temp	Tajima, 1990 [29]
0.767, 0.926, 0.936, 0.965, 1.024, 1.035, 1.071, 1.09, 1.119	1617, 1339, 1325, 1285, 1211, 1198, 1158, 1138, 1108	450°C, 1-200h	15K	Minaev and Mudryi, 1981 [21]
0.767, 0.79, 0.926, 0.97	1617, 1570, 1339, 1279	450°C	18K	Magnea *et al*., 1984 [30]
0.807, 0.817, 0.855, 0.87, 0.920	1537, 1518, 1450, 1425, 1348		12K	Binetti *et al*., 2002 [25]
0.82, 0.85	1512, 1459	650°C, 120h	12K	Leoni *et al*., 2004 [31]
0.957	1296	450°C, 180h	2K	Weman *et al.*, 1985 [32]
1.016 – 1.107	1120 - 1220 several sharp peaks	500°C, 100h	4.2K	Nakayama *et al*., 1981 [33]
1.052, 1.117	1179, 1110	470°C, 60h	4.2K	Liesert *et al*., 1993 [34]
1.085, 1.124, 1.143	1143, 1103, 1085	450°C, 64h	4.2K	Tajima *et al*., 1980 [35]
1.11, 1.16	1117, 1069	430°C	4.2K	Nakayama *et al*., 1980 [20]
1.1128, 1.1143, 1.1163, 1.118		450°C, 80h	4.2K	van Kooten *et al*., 1987 [36]

taken to produce one TDD center, and they concluded that TDD production is a minority process in relation to oxygen precipitation [14]. Previous works have suggested that the formation of thermal donors is enhanced due to self-interstitials emitted by oxygen precipitation [15], [16].

In order to analyze the electronic properties of TDDs and OPs, techniques such as Fourier-transform infrared spectroscopy (FTIR) [10], photoconductance decay [5], [17], and deep-level transient spectroscopy (DLTS) [18], have been applied. Photoluminescence spectroscopy (PLS) is another characterization method that has been used to identify defects including oxygen related defects in Cz-Si [19]–[23]. Both FTIR and photoluminescence are sensitive to the detection of dilute impurities, are non-destructive, and do not require complex sample preparation. In previous studies, high spatial and spectral resolution μPLS measurements have been used to investigate defects, such as oxygen-precipitate related dislocations [24]–[27]. A summary of PL peaks previously observed in silicon wafers containing TDDs, OPs, and defects associated with them, is given in Table I.

In the literature, the PL peak at 1617 nm or 0.767 eV (called the P-line) and several sharp peaks around 1138–1078 nm (1.09–1.15 eV) are primarily observed in samples with TDDs (see Table I). Initially, the photoluminescence emission at 1617 nm (0.767 eV) was ascribed to thermal donors [28]. Later it was shown [25], [34] that this peak occurs as a result of carbon - oxygen complexes. Nakayama *et al.* [20] measured PL spectra at 4.2 K on p-type samples which were annealed for 100 h at 430 °C and found several PL peaks between 1138–1069 nm (1.09 and 1.16 eV), which they associated with oxygen related donors. Similar results were observed by Liesert *et al.* [34]. They also found that the relative intensities of some of these peaks increased with annealing time [20]. Minaev and Mudryi [21], in their PL measurements of n-type silicon wafers at 15 K, observed several peaks between 1771–1127 nm (0.7 and 1.1 eV) which were correlated with thermal donors. The broad peak around 1425 nm (0.87 eV) was attributed to OPs [25]. Since this broad peak overlaps with the well-known dislocation induced D-lines (D1 and D2), extensive work has been performed to distinguish defect luminescence associated with dislocations and oxygen precipitation [27], [37]. However, the broad peak around 1494 nm (0.83 eV) is attributed to defects generated as a result of oxygen precipitation [27], [37]. As given in Table I, most of the photoluminescence measurements have been conducted at the temperature of 4.2–18 K, and the peak centers should change with increasing temperature particularly at 80 K in this article. The peaks around 1617 nm (0.767 eV), 1512 nm (0.82 eV), 1425 nm (0.87 eV), 1339 nm (0.926 eV), 1279 nm (0.97 eV) and between 1107 nm to 1181 nm (1.05–1.12eV) peaks are observed in most of the literature.

TDDs are annihilated by annealing at higher temperatures around 650 °C. Even though TDDs are annihilated, not all defects created during thermal donor generation (TDG) are removed, and some new defects may grow. For example, Basnet *et al.* [7] recently found that ring-like defects grown during TDD generation at 450 °C do not disappear after a TDD annihilation process at 650 °C. Tokuda *et al.* [9] observed similar defect creation using DLTS. The annihilation of TDDs at 650 °C results in only a partial recovery of the interstitial oxygen concentration. It also leads to several new O-related centers [38]. However, there is a lack of clarity as to the exact species formed during TDG, and which species remain after thermal donor annihilation (TDA).

The aim of this article is to quantify the evolution of oxygen related species during TDG and after TDA via PLS. We also investigate the impact of doping type on the evolution of the subbandgap PL spectra with annealing time. However, since increasing concentrations of recombination active defects occur during annealing, the carrier lifetime, and therefore the average injection level, decreases with annealing time when measured with a constant excitation intensity. It has recently been shown that the intensity of the Si band-to-band peak and subbandgap defect-related peaks often have different dependencies on the injection level [39]. This makes it difficult to compare peak intensities across samples with different carrier lifetimes when using a fixed excitation intensity. To avoid this problem, we use a recently demonstrated approach [39], in which the excitation laser intensity is adjusted for each sample, in order to achieve the same band-to-band peak intensity, and therefore the same average injection level. This then allows direct quantitative comparisons of the various peak intensities from sample to sample.

III. Experimental Methods

In this article, eight sister wafers from a phosphorus-doped n-type monocrystalline Cz silicon ingot with an initial O_i concentration $[O_i] = 7.8 \times 10^{17}$ cm^{-3} with starting resistivity of 1 Ω.cm, eight sister wafers from a boron-doped p-type monocrystalline Cz silicon ingot with an initial $[O_i] = 8.6 \times 10^{17}$ cm^{-3} with starting resistivity of 1 Ω.cm, and ten sister wafers from a boron-doped p-type monocrystalline Cz silicon ingot with an initial $[O_i] = 5.5 \times 10^{17}$ cm^{-3} with resistivity 0.8 and 12 Ω.cm were used.

All the samples were etched and cleaned with Radio Corporation of America (RCA) solutions prior to processing. Initially, the samples were annealed at 650 °C for 30 min to remove any pre-existing thermal donors. One n-type and one p-type sample from each set were kept as controls while the remaining samples were annealed at 450 °C for different lengths of time (24, 48, 72, 96, 120, and 144 h) in N_2 gas to create a range of thermal donor concentrations. All the samples were then RCA cleaned again and passivated with silicon nitride (SiN_x) layers via plasma-enhanced chemical vapour deposition (PECVD). During the PECVD process, the samples were inside the chamber for approximately 50 min, reaching a maximum temperature of 300 °C. Compared to the higher temperature and longer durations of the subsequent TDD generation annealing, we expect the amount of TDD generation during the PECVD process to be negligible. The resistivity of each sample was measured with a WCT 120 photoconductance tester from Sinton Instruments [40]. The concentration of thermal donors was determined from the measured change in resistivity, accounting for the fact that TDD are double donors. PL images were captured using an LIS-R1 PL imaging tool from BT imaging [41]. In some samples the TDDs were subsequently annihilated at 650 °C for 30 min in nitrogen.

The thin thermal oxide layers formed during the annealing steps, and the deposited passivation films, were removed by hydrofluoric acid to allow FTIR measurements. $[O_i]$ was measured via the oxygen absorption peak at 1106 cm^{-1} at room temperature via a Bruker Vertex 80 tool and calibrated using the ASTM F121-83 standard with a calibration coefficient of 2.45×10^{17} cm^{-2}. The substitutional carbon concentration $[C_S]$ in the samples was below the detection limit (1.0×10^{16} cm^{-3}) of our FTIR system when measured at room temperature.

PL spectra were measured using a Horiba LabRam micro-PL confocal microscope system with a liquid-nitrogen cooled cryostat to maintain the sample temperature at 80 K. The samples were excited with a supercontinuum laser source (NKT SuperK Extreme EXR-20) with a tunable wavelength. An excitation wavelength of 600 nm with a bandwidth of 10 nm was used. The laser was focused on to the sample surface with a 50× objective lens with a spot size of 1.33 μm in diameter. The emitted PL signal was passed through a monochromator and measured by a liquid-nitrogen-cooled InGaAs detector with detection range from 850 nm to 1600 nm. As described earlier, to generate the same average injection level in all the samples, the power of the tunable laser was adjusted so that all the samples gave the same silicon band-to-band peak intensity. To achieve this, the excitation power was varied from 0.3 to 0.9 mW. Each spectral measurement was taken with an integration time of 10 s. The PL spectra were measured at the same location on each sample, relative to the wafer center, so that the results are comparable across the samples. For the annealed samples, this coincides with the location of the first dark ring from the center. The PL spectra were measured without any surface passivation layers present, in order to avoid potential interference from emission from the passivating films. All PL spectra were corrected for the system's spectral response, which was determined by a calibrated tungsten-halogen light source.

IV. Results and Discussion

A. Resistivity After TDD Generation and Annihilation

Fig. 1 shows the change in resistivity and thermal donor concentration with annealing time for the n-type ($[O_i] = 7.8 \times 10^{17}$ cm^{-3}) and p-type ($[O_i] = 8.6 \times 10^{17}$ cm^{-3}) wafers. As expected, the p-type wafers became n-type due to compensation by the TDDs. The TDD concentration increases rapidly initially, and then begins to saturate after longer annealing times. Both in n-type and p-type samples, after TD annihilation annealing, the resistivity is recovered to the value of the as-grown sample.

B. Loss in $[O_i]$

Fig. 2 shows the evolution of $[O_i]$ in the n-type Cz samples after subjecting them to the TDD generation treatment (450 °C in nitrogen) for 24, 48, 72, 96, 120, and 144 h, and then after a subsequent TDD annihilation (650 °C for 30 min) step.

As expected, we observe a loss in $[O_i]$ with increasing TDD generation duration, due to the sequential clustering of O_i to form different species of TDDs and OPs. In the subsequent TDD annihilation step, we observed a complete recovery of the resistivity as shown in Fig. 1. However, as shown in Fig. 2, we did not observe a corresponding complete recovery of $[O_i]$. This incomplete recovery of $[O_i]$ is attributed to the simultaneous

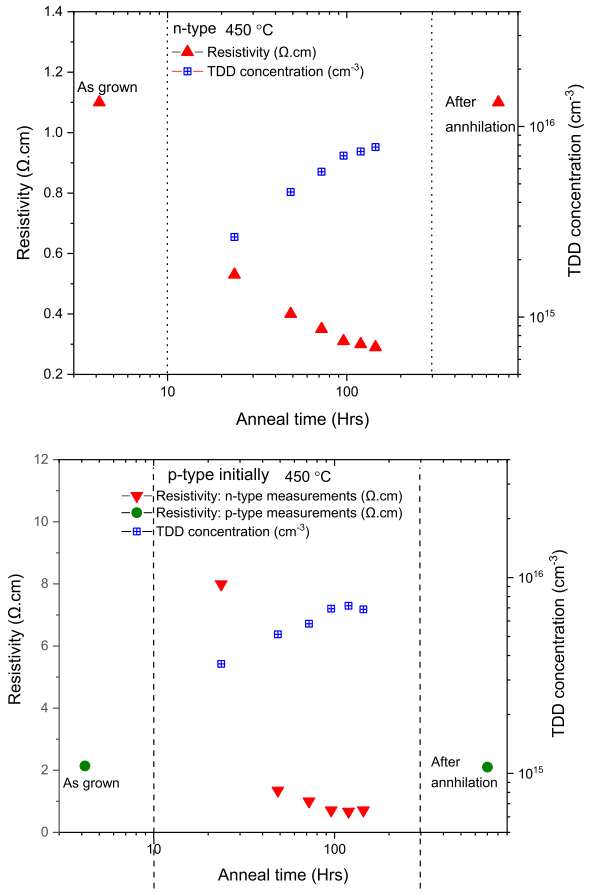

Fig. 1. Evolution of resistivity and TDD concentration of n-type and initially p-type Cz-Si samples. The TDD concentration is determined from the change in resistivity. For the initially p-type samples, the resistivity values shown as red triangles are n-type (compensated) while the green circles are p-type.

formation of OPs during TDD generation, as we have observed previously [7].

C. Band-to-band Photoluminescence Images

In order to observe the impact of thermal donors and OPs on the minority carrier lifetime, Fig. 3 shows uncalibrated band-to-band photoluminescence images of the n-type wafers before TDD generation, after 144 h TDD generation, and after TDD annihilation. Ring like defects formed during TDD generation persist and worsen after TDD annihilation. These samples were passivated with SiN_x and the PL images were measured at 0.87 suns with 2 s illumination time. This confirms prior observations [7] that not only thermal donors, but also recombination-active OPs, are formed at this relatively low temperature.

D. Photoluminescence Spectra

In order to observe the impact of thermal donor and OP formation on subbandgap photoluminescence, the PL spectra were measured in the n-type and p-type wafers with different interstitial oxygen concentrations. Fig. 4 shows the photoluminescence spectra of the n-type and p-type samples annealed for 144 h at 450 °C. Both the polarity and oxygen concentration impact

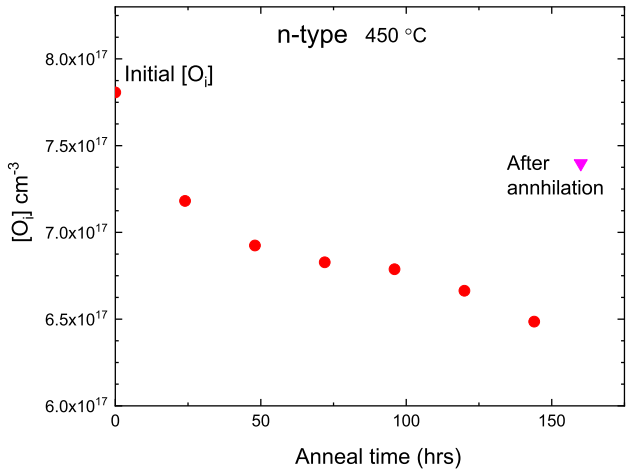

Fig. 2. Measured [O_i] as a function of TDD generation anneal time at 450 °C. The last point (triangle) corresponds to the TDD annihilation step.

the shape and magnitude of the subbandgap photoluminescence peaks.

The much lower magnitude of the subbandgap PL peaks in the p-type samples suggests that the formation of oxygen-related luminescence centers in p-type Si samples is either much slower, or occurs to a much lesser degree, than in n-type silicon at this temperature. Note that this conclusion holds even for the p-type samples with high initial oxygen concentrations. As a result, we focus on the n-type samples for the remainder of this article, for which the PL spectra show strong subbandgap peaks.

As shown in Fig. 5, we identify five different peaks in the n-type Cz-Si samples annealed at 450 °C. These peaks are centered at wavelengths of 1184, 1206, 1249, 1382, and 1420 nm. Later, these spectra are de-convoluted into six Gaussian peaks (see Figs. 6 and 7).

To assess the possible impact of the chosen measurement location on the relative peak intensities, PL spectra were measured at different radial distances on the n-type sample that was annealed for 144 h. The PL spectra measured in the darker and lighter rings showed the same shape as in Fig. 5, but with a changing overall intensity. This suggests that the same defects are present throughout the entire wafer, but are more concentrated in the regions which appear as dark rings in the room temperature PL images. A similar observation on the distribution of OPs was made by Ono *et al.* [42]. Photoluminescence spectra measured on samples passivated with SiN_x films also revealed a very similar spectral shape, although with a much higher intensity due to the surface passivation. This confirms that the detected luminescence arises from the bulk of the wafers, and is not surface-related.

E. Deconvolution of the PL Spectra

In order to and quantify changes in intensity of the various peaks observed, the measured spectra were fitted with a combination of Gaussian subpeaks. Fig. 6 shows the resulting fit of the photoluminescence spectra for the n-type Cz Si wafers before TDG, after TDG (for 144 h annealing), and after TDA. Six peaks

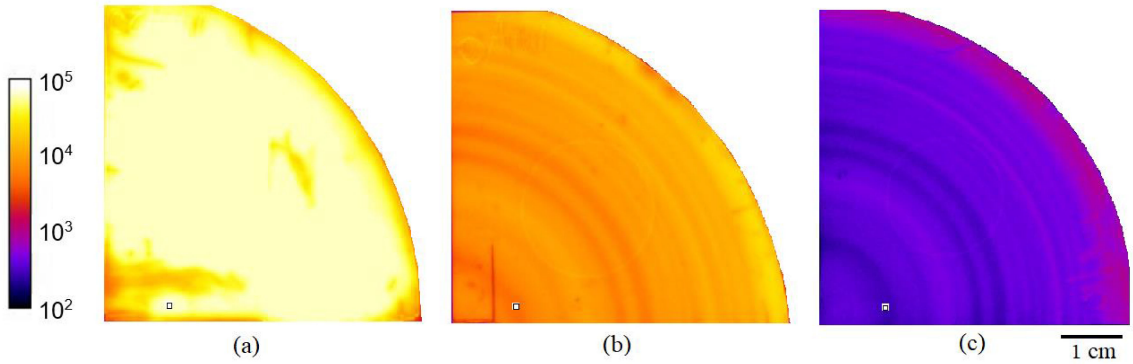

Fig. 3. Uncalibrated photoluminescence images of n-type Cz-Si samples. (a) Before TDD generation. (b) With TDD $= 7.8 \times 10^{15}$ cm^{-3} after annealing at 450 °C for 144 h. (c) After TDD annihilation. The PL counts are shown in a logarithmic scale. The PL spectra were measured at the locations marked with the squares.

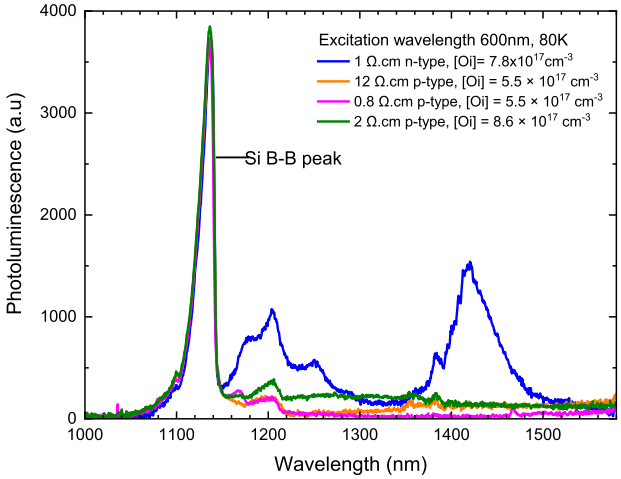

Fig. 4. Photoluminescence spectra (80 K) of n-type and p-type Cz-Si samples after annealing for 144 h at 450 °C.

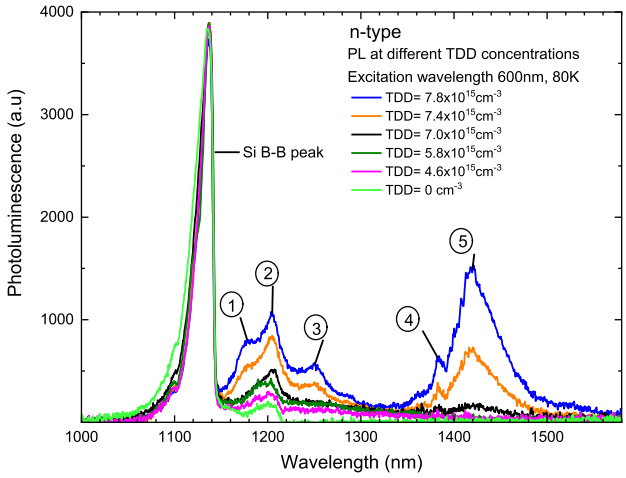

Fig. 5. Photoluminescence spectra (80 K) of n-type Cz-Si samples with increasing thermal donor concentrations (increasing annealing time at 450 °C).

TABLE II
SUMMARY OF PL PEAKS OBSERVED IN THIS ARTICLE

Wavelength (nm)	Previously observed
1184	Minaev and Mudryi, 1981 [21] at 15K
1206	New peak
1249	Minaev and Mudryi, 1981 [21] at 15K
1382	Pizzini *et al.*, 2003 [27] at 12K
1420	Binetti *et al.*, 2002 [25] at 12K
1463	Binetti *et al.*, 2002 [25], Leoni *et al.*, 2004 [31] at 12K

were identified, as given in Table II, which also indicates their relationships to previously observed peaks in the literature.

Here, the spectrum of the sample before TDG was used to extract the shape and height of the phonon replica of the band-to-band peak, which is centered at 1206 nm, as shown in Fig. 7. This is important to take into account, as the oxygen-related peaks at 1184 and 1206 nm overlap with this phonon replica peak. Hence, in further analysis, the phonon replica is included in the spectral fits, so that the oxygen-related peak heights can be accurately determined.

Nakayama *et al.* [33] observed a series of sharp photoluminescence peaks (which they called S_j lines) around 1120–1220 nm, in Cz-Si samples with high interstitial oxygen and substitutional carbon concentrations, annealed at 500 °C. However, these sharp peaks were observed at 4.2 K, but disappeared during measurements at 50 K. Most of these peaks were not observed in samples annealed at lower or higher temperatures, such as 450 °C or 550 °C [33]. The peak we have observed at 1206 nm is therefore likely to be different to the S_j lines observed by Nakayama *et al.* [33].

As shown in Fig. 6–8, after TDA, the 1206 nm peak disappears. Therefore, this peak is most likely related to thermal donors. All the other peaks remain the same or continue to increase after TDA. They are therefore likely related to nanoscale precipitates or precipitate nuclei grown during TDG. Such growth has been observed before [7] albeit not via PLS. Several studies have shown that the generation of defect states or oxygen precipitation is enhanced during annealing at 650 °C when the samples have been pre-annealed at 450 °C, for instance see [3]. In this article, as shown in Fig. 6(c), the peak at 1420 nm

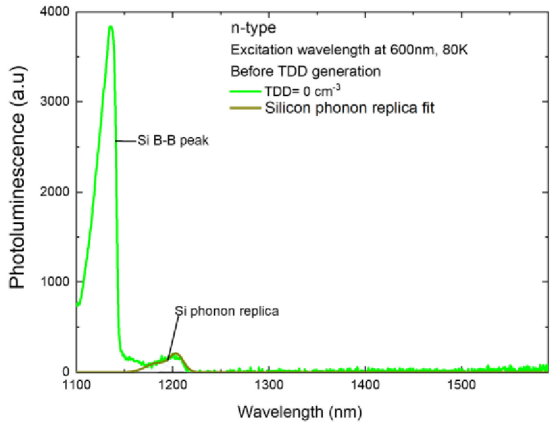

(a)

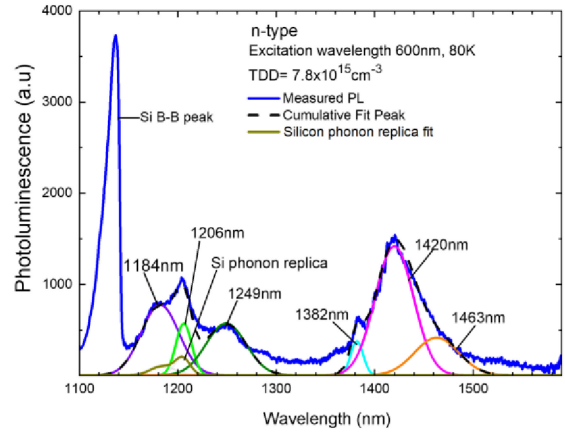

(b)

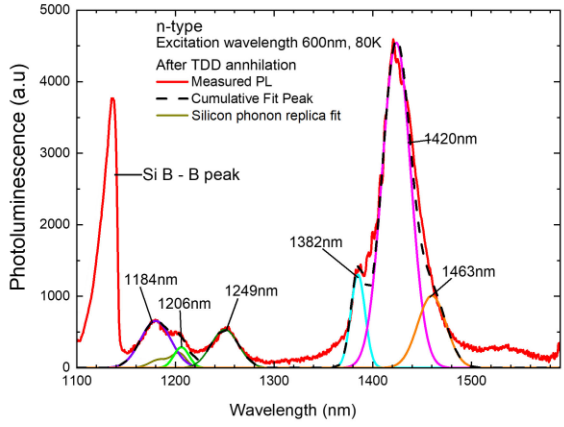

(c)

Fig. 6. Gaussian deconvolution of photoluminescence spectra of n-type Cz-Si samples. (a) Before TDD generation, showing the fitted phonon replica centered at 1206 nm. (b) With a TDD concentration of 7.8×10^{15} cm^{-3} after 144 h annealing at 450 °C. (c) After TDD annihilation.

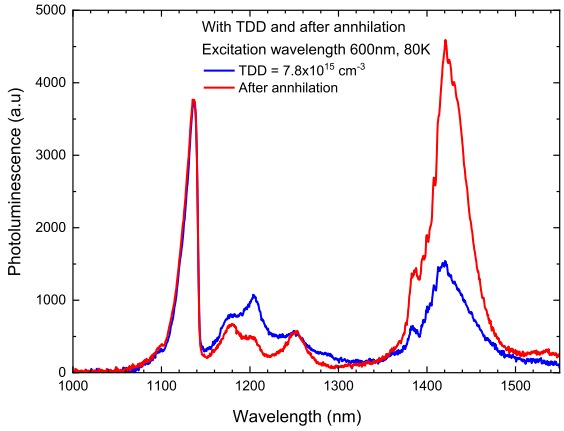

Fig. 7. Photoluminescence spectra (80 K) of the n-type Cz-Si sample with (TDD) $= 7.8 \times 10^{15}$ cm^{-3} before and after TDD annihilation.

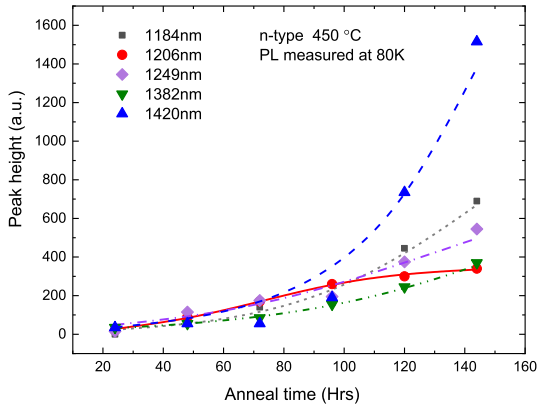

(a)

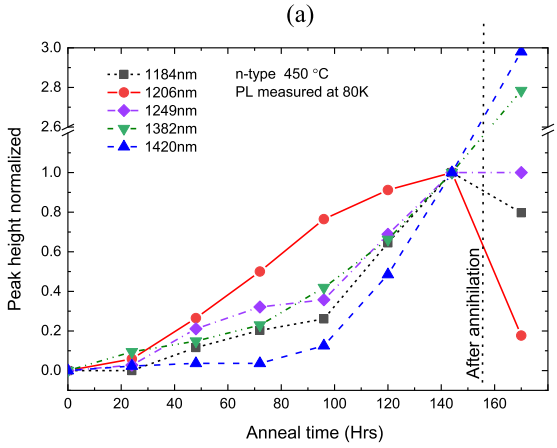

(b)

Fig. 8. Peak height versus annealing time for the n-type Cz-Si samples annealed at 450 °C. (a) Absolute values. (b) Normalized with respect to the peak height after 144 h annealing. In (b), the normalized peak heights after TDA are also given. The lines are guides to the eye.

increased significantly after TDD annihilation by annealing for 30 min at 650 °C. This could be due to enhanced growth of OP during annealing at 650 °C following a 450 °C anneal, and/or that the precipitates become more strained during the 650 °C annealing. For any given nucleation temperature, the density of unstrained precipitates decreases with growth time as they convert into strained precipitates. Strained precipitates are thought more likely to give rise to a detectable subbandgap PL signal in the wavelength range up to 1690 nm [13]. Accordingly, we suggest that the initial loss of $[O_i]$ could be related to the formation of unstrained OPs and then, as the annealing time continues, they convert into strained precipitates, giving rise to subbandgap PL emission [13].

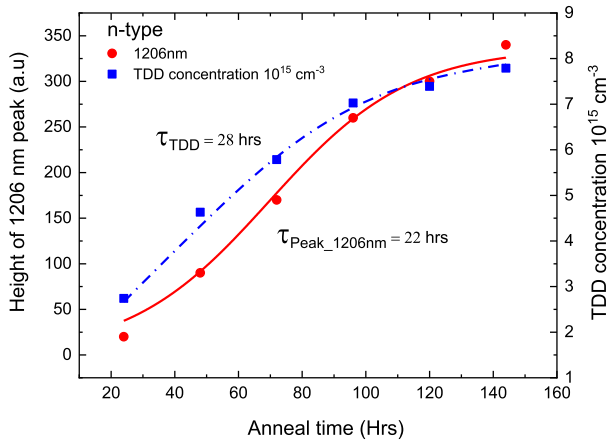

Fig. 9. Height of the peak at 1206 nm (left axis) and thermal donor concentration (right axis) as a function of anneal time at 450 °C. The lines are sigmoidal exponential fits, with the fitted time constants shown.

Previous studies have shown a close correlation between the optical activity of dislocations and the oxygen-related centers. The deconvolution of the broad peak between 1378–1476 nm (0.84–0.9 eV) has been analyzed in several earlier studies, such as [25], [27], [37], and [43]. OPs give rise to a broad PL peak around 1420 nm and this peak increases during a TDD annihilation step at 650 °C. At first glance, this could be attributed to dislocation-related D lines. However, Tajima *et al.* have used microscopic PL mapping to show that this defect band is instead associated with oxygen precipitation [29]. Several other studies have corroborated the result that the broad peak around 1420 nm is attributed to OPs [13], [22], [27], [37] with possible enhanced precipitation around dislocation centers [27], [37]. In this article, we confirm that the peak around 1420 nm is increased with annealing time and the peak is associated with increased OP during the annealing period.

F. Impact of TDA on Photoluminescence Spectra

As shown in Fig. 1, the resistivity recovers to its initial value after TDA (TDA, 30 min annealing at 650 °C). However, after TDA, the peak at 1420 nm continued to increase significantly, while the peak at 1206 nm decreased, as shown in Fig. 7. The other peaks either increased or remained largely unchanged. These results indicate that the broad peak at 1420 nm is not associated with TDDs but with low temperature OP and the ring defects that grow during annealing at 650 °C. On the other hand, the peak at 1206 nm may be more directly related to the presence of TDDs. This correlation is discussed further below.

G. Peak Height Kinetics

The evolution of the various peak heights as a function of annealing time are shown in Fig. 8, as both absolute values [see Fig. 8(a)] and normalized [see Fig. 8(b)]. The normalization was performed relative to the peak heights after 144 h annealing. The 1206 nm peak shows a distinct tapering off after extended annealing times, whereas the other peaks continue to grow rapidly.

In order to confirm that the 1206 nm peak is indeed related to thermal donors, Fig. 9 plots the height of the 1206 nm peak together with the TDD concentration as a function of annealing time. The time constant of the sigmoidal exponential fit for the 1206 nm peak is 20 h whilst the time constant of the thermal donor concentration is 28 h. Hence, the thermal donor concentration grows at a similar rate as the 1206 nm peak, further confirming that the peak at 1206 nm is related to thermal donors. The other peaks, which grow at slower rates, are then considered to be related to the formation of OPs involving increasing numbers of oxygen atoms.

V. Conclusion

Low temperature annealing of silicon wafers at 450 °C creates both thermal donors and OPs. The resulting changes in resistivity are entirely reversible after TDA at 650 °C. However, OP related ring-defects remain after TDA, as evidenced by PL images, and an incomplete recovery of the dissolved oxygen concentration after TDA. PL spectra have been deconvoluted into six distinct PL peaks at low temperatures (80 K) between 1550–1127 nm (0.8–1.1 eV) in n-type silicon wafers. We observe a peak at 1206 nm, (overlapping with the Si phonon replica) which we attribute to thermal donors. The evolution of the height of this peak follows a similar time constant to the TDG. This peak disappears after a TDA step at 650 °C. The other five peaks grow during TDG and remain after TDA. These are most likely related to OPs of increasing size, which grow during TDG. The PL emission characteristics of these five peaks are in agreement with the literature. The peaks at 1249 and 1420 nm are very close to established peaks for OP-related dislocations.

References

[1] M. Claybourn and R. C. Newman, "Activation energy for thermal donor formation in silicon," *Appl. Phys. Lett.*, vol. 51, 1987, Art. no. 2197.
[2] A. G. Steele and M. L. W. Thewalt, "Photoluminescence studies of defects in annealed czochralski silicon," *Can. J. Phys.*, vol. 67, pp. 268–274, 1989.
[3] A. Borghesi, B. Pivac, A. Sassella, and A. Stella, "Oxygen precipitation in silicon," *J. Appl. Phys.*, vol. 77, 1995, Art. no. 4169.
[4] J. A. Hornbeck and J. R. Haynes, *Phys. Rev.*, vol. 100, no. 2, pp. 606–615, 1955.
[5] M. Siriwardhana, Y. Zhu, Z. Hameiri, D. Macdonald, and F. Rougieux, "Photoconductance determination of carrier capture cross sections of slow traps in silicon through variable pulse filling," *IEEE J. Photovolt.*, vol. 11, no. 2, pp. 273–281, Mar. 2021.
[6] M. Tomassini *et al.*, "Recombination activity associated with thermal donor generation in monocrystalline silicon and effect on the conversion efficiency of heterojunction solar cells," *Appl. Phys.*, vol. 119, 2016, Art. no. 084508.
[7] R. Basnet, H. Sio, M. Siriwardhana, F. E. Rougieux, and D. Macdonald, "Ring-like defect formation in n-type Czochralski-grown silicon wafers during thermal donor formation," *Phys. Status Solidi A*, vol. 218, 2021, Art. no. 2000587.
[8] J. Weber and D. I. Bohne, "Passivation thermal donors by At. hydrogen," in *Early Stages of Oxygen Precipitation in Silicon*, New York, NY, USA: Springer, 1996, pp. 123–140.
[9] Y. Tokuda, N. Kobayashi, A. Usami, Y. Inoue, and M. Imura, "Thermal donor annihilation and defect production in n-type silicon by rapid thermal annealing," *J. Appl. Phys.*, vol. 66, 1989, Art. no. 3651.
[10] P. Wagner and J. Hage, "Thermal double donors in silicon," *Appl. Phys. A*, vol. 49, pp. 123–138, 1989.
[11] T. Hallberg and J. L. Lindstrom, "Activation energies for the formation of oxygen clusters related to the thermal donors in silicon," *Mater. Sci. Eng., B*, vol. 36, pp. 13–15, 1996.

[12] W. Kaiser, H. L. Frisch, and H. Reiss, "Mechanism of the formation of donor states in heat-treated silicon," *Phys. Rev.*, vol. 112, no. 5, 1958, Art. no. 1546.
[13] K. Bothe, R. J. Falster, and J. D. Murphy, "Room temperature sub-bandgap photoluminescence from silicon containing oxide precipitates," *Appl. Phys. Lett.*, vol. 101, 2012, Art. no. 032107.
[14] M. Clayboum and R. C. Newman, "Thermal donor formation and the loss of oxygen from solution in silicon heated at 450 °C," *Appl. Phys. Lett.*, vol. 52, 1988, Art. no. 2139.
[15] K. Torigoe and T. Ono, "Formation of thermal donor enhanced by oxygen precipitation in silicon crystal," *AIP Adv.*, vol. 10, 2020, Art. no. 045019.
[16] V. V. Voronkov, "Generation of thermal donors in silicon: Oxygen aggregation controlled by self-interstitials," *Semicond. Sci. Technol.*, vol. 8, 1993, Art. no. 2037.
[17] M. Siriwardhana, D. Macdonald, F. D. Heinz, and F. E. Rougieux, "Slow minority carrier trapping and de-trapping in czochralski silicon: Influence of thermal donors and the doping density," in *Proc. 7th World Conf. Photovoltaic Energy Convers.*, 2018, pp. 3312–3314.
[18] V. P. Markevich *et al.*, "Electron emission and capture by oxygen related bistable thermal double donors in silicon studied with junction capacitance techniques," *J. Appl. Phys.*, vol. 124, 2018, Art. no. 225703.
[19] M. Siriwardhana, F. E. Rougieux, and D. Macdonald, "Defect luminescence from thermal donors in silicon: Impact of dopant type and thermal donor concentration," in *Proc. 47th IEEE Photovolt. Specialists Conf.*, Jun.–Aug., 2020, pp. 2652–2654.
[20] H. Nakayama, J. Katsura, T. Nishino, and Y. Hamakawa, "Hall-Effect and photoluminescence measurements of oxygen-related donors in Cz-Si crystals," *Jpn. J. Appl. Phys.*, vol. 19, no. 9, pp. L547–L550, 1980.
[21] N. S. Minaev and A. V. Mudryi, "Thermally-induced defects in silicon containing oxygen and carbon," *Physica Status Solidi*, vol. 68, pp. 561–565, 1981.
[22] A. Le Donne, S. Binetti, V. Folegatti, and G. Coletti, "On the nature of striations in n-type silicon solar cells," *Appl. Phys. Lett.*, vol. 109, 2016, Art. no. 033907.
[23] R. L. Chin, M. Pollard, Y. Zhu, and Z. Hameiri, "Detailed analysis of radiative transitions from defects in n-type monocrystalline silicon using temperature- and light intensity-dependent spectral photoluminescence," *Sol. Energy Mater. Sol. Cells*, vol. 208, 2020, Art. no. 110376.
[24] S. Pizzini, M. Guzzi, E. Grilli, and G. Borionetti, "The photoluminescence emission in the 0.7–0.9 eV range from oxygen precipitates, thermal donors and dislocations in silicon," *J. Phys., Condens. Matter*, vol. 12, pp. 10131–10143, 2000.
[25] S. Binetti *et al.*, "Optical properties of oxygen precipitates and dislocations in silicon," *J. Appl. Phys.*, vol. 92, 2002, Art. no. 2437.
[26] S. Pizzini, M. Acciarri, E. Leoni, and A. L. Donne, "About the D1 and D2 dislocation luminescence and its correlation with oxygen segregation," *Physica Status Solidi*, vol. 222, pp. 141–150, 2000.
[27] S. Pizzini, E. Leoni, S. Binetti, M. Acciarri, A. Le Donne, and B. Pichaud, "Lumin. Dislocations Oxide Precipitates Si", *Solid State Phenomena*, vol. 95–96, pp. 273–282, 2003.
[28] M. Tajima, P. Stallhofer, and D. Huber, "Deep level luminescence related to thermal donors in silicon," *Jpn. J. Appl. Phys.*, vol. 22, no. 9, pp. L586–L588, 1983.
[29] M. Tajima, "Characterization of semiconductors by photoluminescence mapping at room temperature," *J. Cryst. Growth*, vol. 103, pp. 1–7, 1990.
[30] N. Magnea, A. Lazrak, and J. L. Pautrat, "Luminescence of carbon and oxygen related complexes in annealed silicon," *Appl. Phys. Lett.*, vol. 45, pp. 60–62, 1984.
[31] E. Leoni, L. Martinelli, S. Binetti, G. Borionetti, and S. Pizzini, "The origin of photoluminescence from oxygen precipitates nucleated at low temperature in semiconductor silicon," *J. Electrochem. Soc.*, vol. 151, no. 12, pp. G866–G869, 2004.
[32] H. Weman, B. Monemar, and P. O. Holtz, "Neutral carbon-related complex defects and the annealing of thermal donors in p-type czochralski silicon," *Appl. Phys. Lett.*, vol. 47, 1985, Art. no. 1110.
[33] H. Nakayama, T. Nishino, and Y. Hamakawa, "Luminescence of thermally induced defects in si crystals," *Appl. Phys. Lett.*, vol. 38, p. 623, 1981.
[34] B. J. H. Liesert, T. Gregorkiewicz, and C. A. J. Ammerlaan, "Photoluminescence of silicon thermal donors," *Phys. Rev. B, Condens. Matter*, vol. 47, no. 12, pp. 7005–7012, 1993.
[35] M. Tajima, S. Kishino, M. Kanamori, and T. Iizuka, "Photoluminescence analysis of annealed silicon crystals," *J. Appl. Phys.*, vol. 51, 1980, Art. no. 2247.
[36] J. J. van Kooten, T. Gregorkiewiczi, A. J. Blaakmeer, and C. A. J. Ammerlaan, "Photoluminescence on oxygen-rich acceptor-doped silicon," *J. Phys. C, Solid State Phys.*, vol. 20, pp. 2183–2191, 1987.
[37] M. Tajima, M. Tokita, and M. Warashina, "Photoluminescence due to oxygen precipitates distinguished from the D lines in annealed si," *Mater. Sci. Forum*, vol. 196–201, pp. 1749–1754, 1995.
[38] L. I. Murin, J. L. Lindstrom, V. P. Markevich, A. Misiuk, and C. A. Londos, "Thermal double donor annihilation and oxygen precipitation at around 650 °C in Czochralski-grown si: Local vibrational mode studies," *J. Phys., Condens. Matter*, vol. 17, pp. S2237–S2246, 2005.
[39] R. Basnet, M. Siriwardhana, H. Nguyen, and D. MacDonald, "Impact of gettering and hydrogenation on sub-band-gap luminescence from ring defects in Czochralski-grown silicon," *ACS Appl. Energy Mater.*, vol. 4, no. 10, pp. 11258–11267, 2021.
[40] R. A. Sinton, A. Cuevas, and M. Stuckings, "in *Proc. 25th IEEE Photovolt. Specialists Conf.*, 1996, pp. 457–460.
[41] T. Trupke, R. Bardos, M. Schubert, and W. Warta, "Photoluminescence imaging of silicon wafers," *Appl. Phys. Lett.*, vol. 89, no. 4, pp. 044107–044107, 2006.
[42] H. Ono, T. Ikarashi, S. Kimura, and A. Tanikawa, "Anomalous ring-shaped distribution of oxygen precipitates in a Czochralski grown silicon crystal," *J. Appl. Phys.*, vol. 78, 1995, Art. no. 4395.
[43] S. Binetti, A. Le Donne, and A. Sassella, "Photoluminescence and infrared spectroscopy for the study of defects in silicon for photovoltaic applications," *Sol. Energy Mater. Sol. Cells*, vol. 130, pp. 696–703, 2014.